Dalton Transactions

ROYAL SOCIETY OF CHEMISTRY

COMMUNICATION

View Article Online
View Journal | View Issue

Cite this: *Dalton Trans.*, 2025, **54**, 9483

Received 15th April 2025,
Accepted 25th May 2025

DOI: 10.1039/d5dt00894h

rsc.li/dalton

Synthesis and characterization of Al and Si substituted polyoxometalates†

Jan-Christian Raabe, [a,b] Saurabh S. Chitnis [b] and Maximilian J. Poller *[a]

Polyoxometalates with different transition-metals substituting the main framework element have recently been applied as promising catalysts. In comparison, polyoxometalates, featuring main-group elements in their framework are extremely rare. In this work, we present two main-group element substituted Keggin-type phosphotungstates containing Al or Si, and their characterization using spectroscopic and crystallographic methods. Al substituted POMs are rare examples, which means that the investigation of such systems deserves special attention. Guided by electronic-structure calculations, the reactivity of the Al substituted cluster with the electrophile benzyl bromide was investigated. This reactivity study together with the results of computational simulations illustrate new reaction behaviour for main-group element substituted polyoxometalates, setting the stage for future applications.

Polyoxometalates (POMs) are inorganic polyanionic cluster compounds, formed by transition-elements of group five (V, Nb, Ta) and six (Mo, W) of the periodic table, mostly in their highest oxidation states.[1] Formally, POMs can be understood as oxometal complexes, in which the oxo ligand can coordinate the metal M in a terminal M=O or two metals in a bridging bond motif M–O–M (Fig. S1, ESI†).[2–4] In general, the M–O units form defined octahedra MO_6, that are connected *via* common edges or corners during POM formation. POM formation corresponds to the formation of M–O–M bonds, so-called bridging of metals by oxo ligands, and is achieved in an acidic medium. A cleavage of these bonds is possible in a basic reaction medium. A POM structure can be decomposed here to so-called monometallates MO_4^{2-}. However, a controlled decomposition of the cluster is also possible in basic reaction media, where individual MO_4^{2-} anions are selectively released from the cluster. So-called defects or vacancies remain in the POM structure. Such structure-types are called Lacunary-type structures and are known for Keggin– and Wells–Dawson-type POM structures. Thus, intact POM structures can be distinguished from those of the defect structures (Lacunary-type). Lacunary-type structures therefore do not represent a separate structure-type but can be derived from any POM-type structure.

A large variety of structure-types for POMs are known (Fig. S2, ESI†).[1,5] The most important one is the Keggin-type ($[XM_{12}O_{40}]^{n-}$), with a heteroelement X at the centre of its structure.[6] The framework metals M are usually Mo and W, but can be partially substituted.[1,7–15] Fundamentally, there are four distinct atom positions in a Keggin-type POM molecule: the heteroelement position (usually main-group elements like P, Si, S, Sb, or Te), the framework-element position (mostly Mo, W including foreign-elements), the oxo ligands, and the cations compensating the charge (Fig. S3, ESI†).[6,16–18] POMs with hard cation such as protons or light alkali cations are known for their high water solubility.[19] In contrast, soft cations such as Cs^+, form POM salts that are insoluble practically all solvents.[20,21] To achieve solubility in organic solvents, POMs can also be combined with organic cations, such as tetrabutylammonium (TBA). These organic cation salts are soluble in polar organic solvents such as acetonitrile (Fig. S4, ESI†). With this strategy, the POM chemistry can be successfully transferred from aqueous to the organic reaction media.[22–25]

Foreign-element substitution in POM chemistry is an emerging and active research field that significantly diversifies the composition and structural possibilities. Selective substitution of one or more framework-elements by different transition-elements like vanadium, niobium, or cobalt, give the POM cluster new electronic properties, making POMs interesting candidates for applications in the fields of biomedicine or catalysis.[26–33] Most examples of foreign-element substituted POMs contain different transition-metals in the framework-element position. In contrast, only few examples are known

[a]*Institute for Technical and Macromolecular Chemistry, Universität Hamburg, Bundesstraße 45, 20146 Hamburg, Germany.*
E-mail: JanChristian.Raabe@uni-hamburg.de, Maximilian.Poller@uni-hamburg.de
[b]*Department of Chemistry, Dalhousie University, Coburg Road 6274, 15000 Halifax, Nova Scotia, Canada. E-mail: Jan-Christian.Raabe@dal.ca, Saurabh.Chitnis@dal.ca*

†Electronic supplementary information (ESI) available. CCDC 2441126. For ESI and crystallographic data in CIF or other electronic format see DOI: https://doi.org/10.1039/d5dt00894h

with main-group elements incorporated in the POM structure in positions other than the central heteroelement.[18] The majority of these are POMs with main-group cations,[34,35] which sometimes form coordination polymers, in which the individual POM clusters are linked *via* coordination to main-group element cations.[36–40] Incorporation of main-group elements as substitutional elements into the framework-element position is extremely rare.[41]

Given the increasing importance of transition-metal substituted POMs, we believe that expanding this concept to main-group substituted POMs is a promising step towards a more versatile application of main-group elements. Therefore, we investigated the incorporation of two elements (Al and Si) into the Keggin-type phosphotungstate structure, utilizing organoammonium salts to enable the use of moisture sensitive main-group precursors in organic solvents.

We started from a Lacunary–Keggin-type POM structure with a defined number of vacancies, as a precursor. The anion $[PW_9O_{34}]^{9-}$ was initially synthesized from phosphate and tungstate.[42] Tungsten was chosen as the framework-element, as W-based POM structures are generally more stable than Mo-based structures. This becomes clear from the Mo-based Lacunary–Keggin-type POM $[PMo_9O_{34}]^{9-}$, which tends to dimerize.[28,43] However, since most of the main-group element precursors required (aluminum trichloride and tetraethyl orthosilicate, TEOS) are sensitive to hydrolysis, the Lacunary-POM precursor was precipitated from aqueous solution with TBA cations and transferred to acetonitrile. Within the anhydrous organic medium, a precursor for the main-group element (1 equivalent) and WO_4^{2-} precursor for the framework-element (2 equivalents) were added stoichiometrically to the Lacunary-type structure $[PW_9O_{34}]^{9-}$, generating the fully intact Keggin-type structure. This strategy for obtaining main-group element-substituted POMs is illustrated in Fig. 1.

The resulting products were analysed with ICP-OES and C, H, N analysis to determine their elemental composition (Table 1 and Table S1†).

For both, **PAlW** and **PSiW**, we found P, Al, Si, and W in the expected ratios, indicating successful integration of Al and Si respectively. If the main-group elements are incorporated into the framework-element position, we would expect anionic charges of −6 for **PAlW** and −5 for **PSiW**. The reduced values for C/H/N could indicate that the negative charge of the anions is not compensated by the TBA cations alone, but additional protons might be present, resulting in acidic compounds of the type $TBA_xH_{n-x}[PMW_{11}O_{40}]$. Stoichiometrically, four TBA cations and two protons are present for POM **PAlW** and 3.37 TBA cations and 1.63 protons for POM **PSiW**, which compensate for the anionic charges of −6 (**PAlW**) and −5 (**PSiW**). This results in stoichiometric formulas of $(TBA)_4H_2[PAlW_{11}O_{40}]$ and $(TBA)_{3.37}H_{1.63}[PSiW_{11}O_{40}]$. The remaining protons originate from the acidic pH medium during the synthetic procedure and protonate the terminal oxo ligands.[44] Interestingly, 4.623 TBA cations were found for the precursor, the anion $[PW_9O_{34}]^{9-}$, with the rest of the ninefold anionic charge having to be balanced by 4377 protons. This results in a stoichiometric molecular formula of $(TBA)_{4.623}H_{4.377}[PW_9O_{34}]$. The raw data of the elemental analysis (CHNS and ICP-OES) can be found in the ESI† under the respective experimental procedures, chapter 2.2.

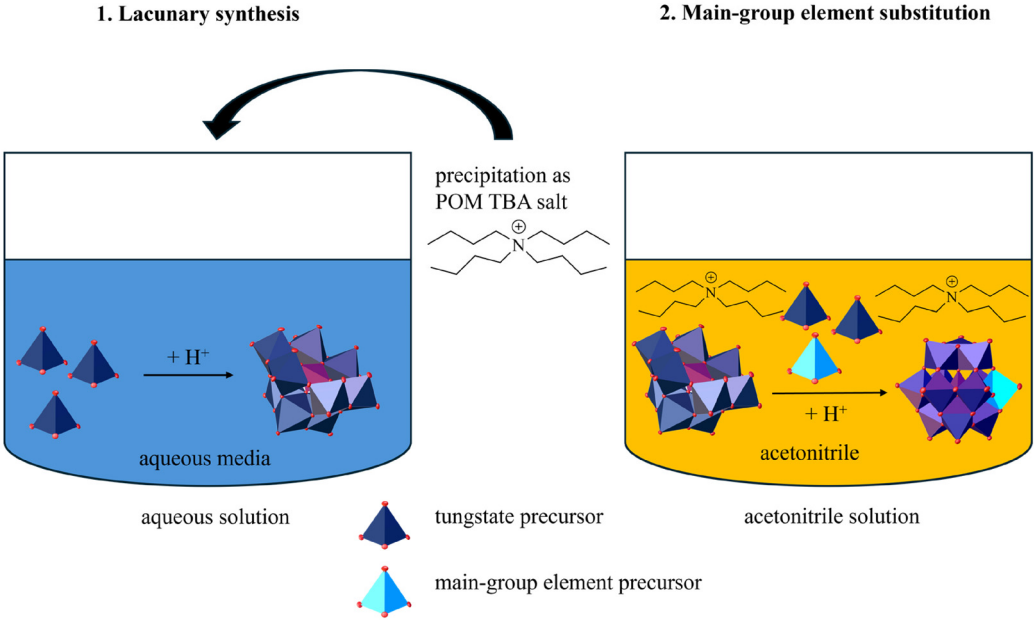

Fig. 1 Synthetic strategy used in this work for the main-group element substitution in POMs. The Lacunary-type structure was synthesized in aqueous media and was directly precipitated as TBA salt. Main-group element substitution experiments were done in acetonitrile solution, using the TBA modified lacunary-type POM and a main-group element precursor.

Table 1 Results from elemental analysis for the Al and Si substituted Keggin-type structures. The stoichiometric ratios were verified by ICP-OES (P, Al, Si, W) and CHNS (C, H, N)

POM	Expected stoichiometry	Cations found	P	Al	Si	W
***n*Bu$_4$NPW**	3 $(C_{16}H_{36}N)^+$ $[PW_{12}O_{40}]^{3-}$	3.00 $(C_{16}H_{36}N)^+$	1.04	—	—	12.0
***n*Bu$_4$NPAlW**	6 $(C_{16}H_{36}N)^+$ $[PAlW_{11}O_{40}]^{6-}$	4.00 $(C_{16}H_{36}N)^+$	1.09	0.916	—	11.0
***n*Bu$_4$NPSiW**	5 $(C_{16}H_{36}N)^+$ P/Si/W $[PSiW_{11}O_{40}]^{5-}$	3.37 $(C_{16}H_{36}N)^+$	0.927	—	0.818	11.0

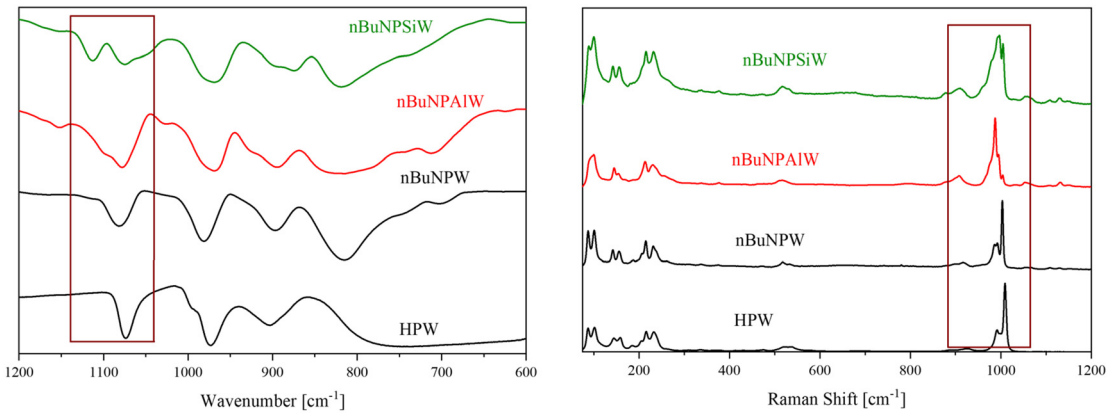

Fig. 2 IR (left) and Raman data (right) of all investigated POMs, compared to the POM acid **HPW** without TBA cation modification.

The integrity of the structure-types was verified by KBr-IR and Raman spectroscopy. All spectra are shown in Fig. 2 and S5–S7 in the ESI.† IR/Raman data in Fig. 2 were compared to unsubstituted POM acid $H_3[PW_{12}O_{40}]$ (abbreviated as **HPW**), which contains significant amounts of hydration water (peaks in IR at 1613 and 3134 to 3650 cm^{-1}).[45] Both main-group element substituted POMs show splitting of the P–O vibrational bands, indicating reduced symmetry.

If the IR spectrum of POM **PSiW** is compared with that of the commercially available $H_4[SiW_{12}O_{40}]$ (**SiW**), it can be concluded that the Si(IV) atom has not substituted the heteroelement position, since no split Si–O band would be expected for $[SiW_{12}O_{40}]^{4-}$ (see Fig. S8, ESI†).

Using single-crystal X-ray diffraction (sc-XRD) the solid-state structure of compound **PAlW** was investigated, as shown in Fig. 3. In agreement with the vibrational data the solid-state structure was identified as a disordered (inversion at P1) Keggin-type anion. A short discussion for the refinement details is provided in the ESI† together with a justification of the atom assignement (see Fig. S9†). Table S2† shows observed bond lengths in comparison to the sum of covalent radii.[46] A comparison of the bond lengths with those of the anion $[PW_{12}O_{40}]^{3-}$ shows (see ESI†) that in particular the O_1–M_1 and M_1–O_2 bond lengths in **PAlW** are shortened by 0.039 and 0.019 Å, which indicates that the Al atom is incorporated into the framework-element position.

For further confirmation of the successful incorporation of Al, the product was investigated using ^{31}P and ^{27}Al NMR spectroscopy and electrochemistry, as shown in Fig. S11–S20, S29 and S30, ESI.† In the ^{27}Al NMR data (Fig. S29†), a peak at 103.8 ppm was identified, indicating that the Al atom is located in a tetrahedral environment.[47] This is contrary to the other analytical findings. However, we believe it can be explained by dissociation of the Al in solution, a behaviour which is commonly observed in transition-metal substituted POMs.[28–30]

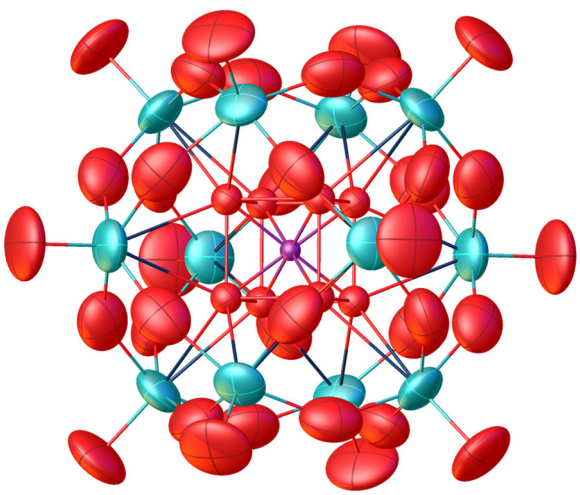

Fig. 3 Refinement of the crystallographic data of anion PAlW in $Im\bar{3}m$. Color code: red – oxygen (ligand position), purple – phosphorous (heteroelement position) and turquoise – metals (W, Al; framework-element position). R_1: 5.71%, wR_2: 10.46%, GooF: 1.052 and R_{int}: 9.58%. Full .cif file is available through the joint Cambridge Crystallographic Data Centre and Fachinformationszentrum Karlsruhe Access Structures service (deposition number: 2441126†).

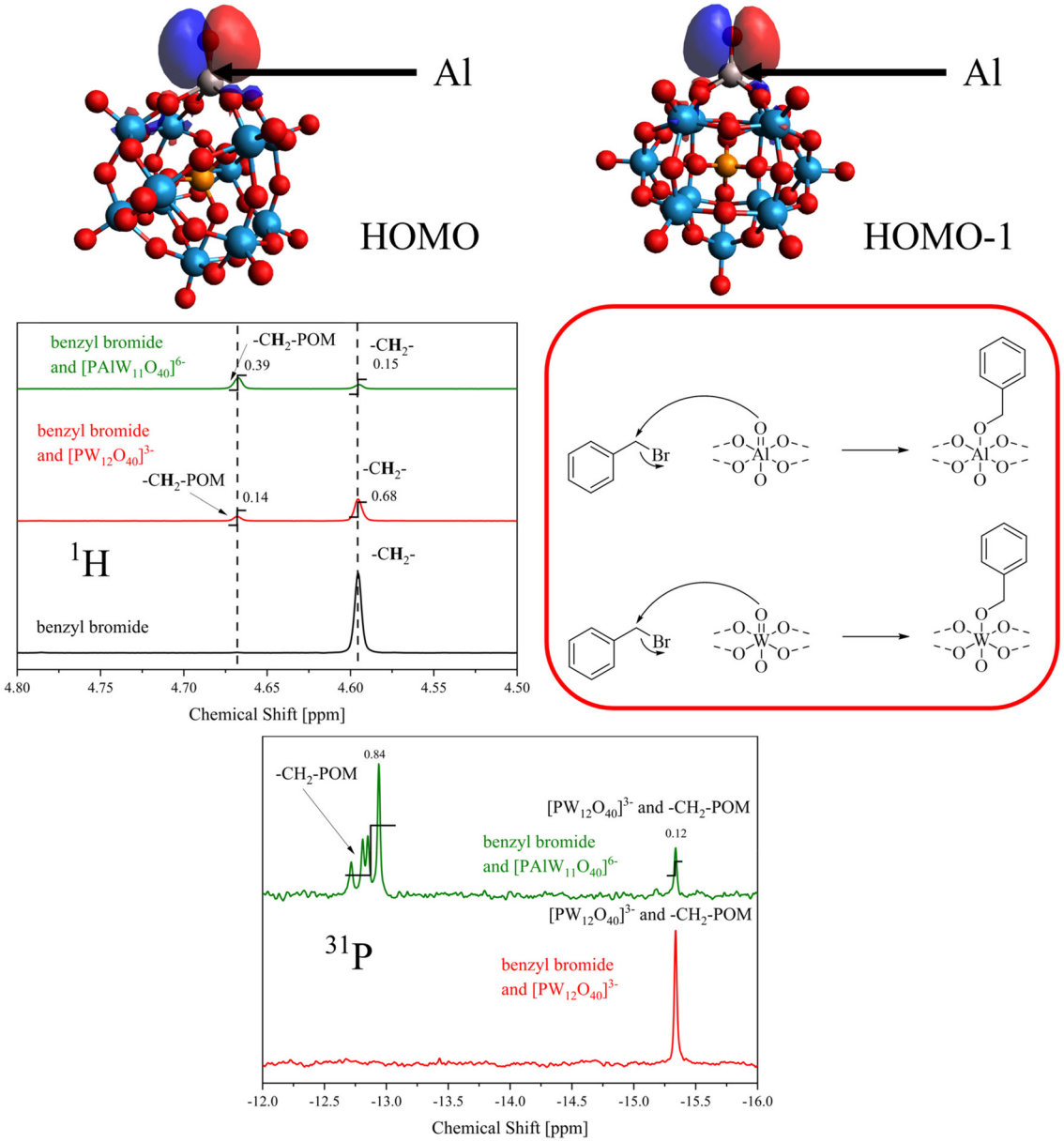

Fig. 4 Reactivity study of compound ***n*Bu$_4$NPW** and ***n*Bu$_4$NPAlW** with benzyl bromide. HOMO (top left) and HOMO−1 (top right) of POM **PAlW**. ^{1}H NMR (middle left) with the shift of the –CH_2– protons. The spectrum was measured at 400 MHz using tetramethyl silane in chloroform as reference (0 ppm). ^{31}P NMR (bottom) of the modified POMs. The spectrum was measured at 161.9 MHz using aqueous H_3PO_4 solution as reference (0 ppm). All spectra were measured in acetonitrile-*d*3 solution.

From our DFT calculations we were able to see, in comparison to POM **PW**, that the HOMO and HOMO−1 are strongly localized on the terminal oxygen atom of the main-group foreign-element (Fig. 4, top), if we assume that one of the tungsten framework-elements has been successfully replaced with Al. This observation implies that this oxygen atom acts as a nucleophile and could react with the LUMO of a suitable electrophile. For POM **PW** an **AlW**, both the HOMO and the HOMO−1 appear to be delocalized over the entire cluster (Fig. S31 and S32†). Therefore, benzyl bromide was added to a solution of ***n*Bu$_4$NPAlW** and ***n*Bu$_4$NPW** in acetonitrile. The solution was then analyzed with ^{1}H, ^{13}C and ^{31}P NMR, as shown in Fig. 4 (bottom).

The ^{1}H NMR in Fig. 4 (middle left) clearly shows a shift of the –CH_2– protons of the benzyl bromide to higher values. While the –CH_2– protons of the benzyl bromide appear at 4.60 ppm, the –CH_2– protons of the benzyl bromide-modified POMs **PW** and **PAlW** each have a peak at 4.67 ppm with different intensities. These results suggest that the unsubstituted POM **PW** is also reactive, but to a lesser extent than **PAlW**, which is consistent with the DFT prediction that the molecular orbitals HOMO−1 and HOMO of the former are

both delocalized over the entire cluster (see experimental procedure ESI, 2.2.6†). For POM **PAlW**, the peak at 4.67 ppm is significantly more intense, which agrees with the DFT prediction for a higher degree of reactivity at the terminal oxo ligand of the Al atom. For both POMs it was also shown that unreacted benzyl bromide is still present, which means that the conversion is not complete. From the integrals, the ratio of modified to unmodified POM is 0.206 for **PW** and 2.6 for **PAlW**, which is consistent with the predicted higher reactivity at the oxo ligand from Al. Similar observations were also made in the ^{31}P NMR data (bottom right). After the addition of benzyl bromide to the terminal oxo ligand of Al, the nucleophilicity of the POM anion could increase, resulting in multiple addition of benzyl bromide to other terminal oxo ligands of W. Therefore, several signals can be seen in the ^{31}P NMR in Fig. 4 (bottom). The complete NMR spectra can be found in the ESI, Fig. S21–S28.† It can be concluded from the discussion of the elemenal analysis that further protons are present in the solid-state structure of the POM anions **PAlW** and **PSiW**, which protonate the terminal oxo ligands. From the discussion presented here, it can be concluded that the protons preferentially occupy the terminal oxo ligands that contain the foreign-elements, as their nucleophilicity is significantly increased.[44]

From the collected data, it can be concluded that the main-group elements Al and Si can be successfully incorporated into the Keggin-type POM structure. The vibrational spectra clearly indicate a successful incorporation of those elements in the position of the framework element. ^{27}Al NMR measurements show a tetrahedrally coordinated Al, which indicates dissociation of the Al substituted POM in solution. DFT calculations predicted high nucleophilic reactivity at the Al atom for an $[PAlW_{11}O_{40}]^{6-}$ anion, as the HOMOs are much more delocalized for $[PW_{12}O_{40}]^{3-}$. This reactivity has been experimentally verified by a reaction with benzyl bromide. Thereby it is confirmed that adding an electropositive main-group metal as the foreign-element is that the HOMO becomes localized at the substitution site, allowing for well-defined reactions and enhanced nucleophilicity relative to unsubstituted derivatives. Thus, main-group substitution presents a highly promising strategy to introduce special reactivity to Keggin-type POMs, revealing a new frontier in the chemistry of the main group elements. Collectively, these synthetic, structural, and reactivity studies provide a foundation for more application focussed studies into main-group and transition-metal hybrid HPAs in the future.

Author contributions

Jan-Christian Raabe: writing – original draft, review & editing, investigation, conceptualization, methodology, visualization. Saurabh Chitnis: conceptualization, methodology, resources, supervision, writing – original draft, review & editing, funding acquisition. Maximilian J. Poller: conceptualization, methodology, supervision, project administration, writing – original draft, review & editing.

Data availability

The full crystallographic information is available as a .cif file through the joint Cambridge Crystallographic Data Centre and Fachinformationszentrum Karlsruhe Access Structures service (deposition number: 2441126†).

Conflicts of interest

The authors declare no conflict of interest.

Acknowledgements

The authors gratefully thank MITACS (the Mathematics of Information Technology and Complex Systems) for financing Jan-Christian Raabe with a Mitacs Globalink Research Award to Canada. We thank all analytical departments that were involved in our project.

References

1 R. Dehghani, S. Aber and F. Mahdizadeh, *Clean: Soil, Air, Water*, 2018, **46**, 1800413.
2 M. T. Pope and A. Müller, *Angew. Chem.*, 1991, **103**, 56–70.
3 J. J. Borrás-Almenar, E. Coronado, A. Müller and M. Pope, *Polyoxometalate Molecular Science*, Springer Netherlands, Dordrecht, 2003.
4 H. J. Lunk and H. Hartl, *ChemTexts*, 2021, **7**, 1–30.
5 M. T. Pope and A. Müller, *Angew. Chem., Int. Ed. Engl.*, 1991, **30**, 34–48.
6 J.-C. Raabe, F. Jameel, M. Stein, J. Albert and M. J. Poller, *Dalton Trans.*, 2024, **53**, 454–466.
7 J. F. Keggin, *Nature*, 1933, **131**, 908–909.
8 M. X. Xu, S. Lin, L.-M. Xu and S.-L. Zhen, *Transition Met. Chem.*, 2004, **29**, 332–335.
9 L. M. Sanchez, Á. G. Sathicq, G. T. Baronetti, H. J. Thomas and G. P. Romanelli, *Catal. Lett.*, 2014, **144**, 172–180.
10 I.-M. Mbomekalle, Y. W. Lu, B. Keita and L. Nadjo, *Inorg. Chem. Commun.*, 2004, **7**, 86–90.
11 A. F. Wells, *Structural Inorganic Chemistry*, Oxford, 1984.
12 B. Dawson, *Acta Crystallogr.*, 1953, **6**, 113–126.
13 J. S. Anderson, *Nature*, 1937, **140**, 1937.
14 H. T. Evans, *J. Am. Chem. Soc.*, 1948, **70**, 1291–1292.
15 H. T. Evans, *Inorg. Chem.*, 1966, **5**, 967–977.
16 A. Patel, N. Narkhede, S. Singh and S. Pathan, *Catal. Rev. - Sci. Eng.*, 2016, **58**, 337–370.
17 J. Breibeck, N. I. Gumerova and A. Rompel, *ACS Org. Inorg. Au*, 2022, **2**, 477–495.
18 K. Y. Monakhov, C. Gourlaouen, R. Pattacini and P. Braunstein, *Inorg. Chem.*, 2012, **51**, 1562–1568.
19 A. Misra, K. Kozma, C. Streb and M. Nyman, *Angew. Chem.*, 2020, **132**, 606–623.
20 D. J. Sures, S. K. Sahu, P. I. Molina, A. Navrotsky and M. Nyman, *ChemistrySelect*, 2016, **1**, 1858–1862.

21 D. J. Sures, P. I. Molina, P. Miró, L. N. Zakharov and M. Nyman, *New J. Chem.*, 2016, **40**, 928–936.
22 C. Li, N. Mizuno, K. Yamaguchi and K. Suzuki, *J. Am. Chem. Soc.*, 2019, **141**, 7687–7692.
23 C. Li, K. Yamaguchi and K. Suzuki, *Chem. Commun.*, 2021, **57**, 7882–7885.
24 Y. Koizumi, K. Yonesato, K. Yamaguchi and K. Suzuki, *Inorg. Chem.*, 2022, **61**, 9841–9848.
25 D. Gabb, C. P. Pradeep, T. Boyd, S. G. Mitchell, H. N. Miras, D.-L. Long and L. Cronin, *Polyhedron*, 2013, **52**, 159–164.
26 J. C. Raabe, J. Albert and M. J. Poller, *Chem. – Eur. J.*, 2022, **28**, e202201084.
27 S. D. Mürtz, J.-C. Raabe, M. J. Poller, R. Palkovits, J. Albert and N. Kurig, *ChemCatChem*, 2024, **16**, e202301632.
28 J.-C. Raabe, T. Esser, F. Jameel, M. Stein, J. Albert and M. J. Poller, *Inorg. Chem. Front.*, 2023, **10**, 4854–4868.
29 J.-C. Raabe, J. Aceituno Cruz, J. Albert and M. J. Poller, *Inorganics*, 2023, **11**, 138.
30 J.-C. Raabe, M. J. Poller, D. Voß and J. Albert, *ChemSusChem*, 2023, **16**, 2013–2015.
31 J.-C. Raabe, L. Hombach, M. J. Poller, A. Collauto, M. M. Roessler, A. Vorholt, A. K. Beine and J. Albert, *ChemCatChem*, 2024, **16**, e202400395.
32 M. J. Poller, S. Bönisch, B. Bertleff, J.-C. Raabe, A. Görling and J. Albert, *Chem. Eng. Sci.*, 2022, **264**, 118143.
33 T. Esser, A. Wassenberg, J. Raabe, D. Voß and J. Albert, *ACS Sustainable Chem. Eng.*, 2024, **12**, 543–560.
34 H. Aliyan, R. Fazaeli and N. Habibollahi, *J. Korean Chem. Soc.*, 2012, **56**, 591–596.
35 I. C. B. Martins, D. Al-Sabbagh, U. Bentrup, J. Marquardt, T. Schmid, E. Scoppola, W. Kraus, T. M. Stawski, A. Guilherme Buzanich, K. V. Yusenko, S. Weidner and F. Emmerling, *Chem. – Eur. J.*, 2022, **28**, e202200079.
36 N. Ncube, S. Bhattacharya, D. Thiam, J. Goura, A. S. Mougharbel and U. Kortz, *Eur. J. Inorg. Chem.*, 2019, **2019**, 363–366.
37 R. Khoshnavazi, L. Bahrami and M. Rezaei, *RSC Adv.*, 2017, **7**, 45495–45503.
38 T. Hanaya, K. Suzuki, R. Sato, K. Yamaguchi and N. Mizuno, *Dalton Trans.*, 2017, **46**, 7384–7387.
39 L. Bahrami, R. Khoshnavazi and A. Rostami, *J. Coord. Chem.*, 2015, **68**, 4143–4158.
40 S. Matsunaga, T. Otaki, Y. Inoue, K. Mihara and K. Nomiya, *Inorganics*, 2016, **4**, 16.
41 Z. Han, H. Zhang, J. Yan and X. Zhai, *Dalton Trans.*, 2016, **45**, 14044–14048.
42 R. G. Finke, M. W. Droege and P. J. Domaille, *Inorg. Chem.*, 1987, **26**, 3886–3896.
43 C. Marchal-Roch, E. Ayrault, L. Lisnard, J. Marrot, F.-X. Liu and F. Sécheresse, *J. Cluster Sci.*, 2006, **17**, 283–290.
44 D.-L. Long, C. Streb, Y.-F. Song, S. Mitchell and L. Cronin, *J. Am. Chem. Soc.*, 2008, **130**, 1830–1832.
45 V. Sasca, M. Stefanescu and A. Popa, *J. Therm. Anal. Calorim.*, 2003, **72**, 311–322.
46 P. Pyykkö and M. Atsumi, *Chem. – Eur. J.*, 2009, **15**, 186–197.
47 M. Haouas, F. Taulelle and C. Martineau, *Prog. Nucl. Magn. Reson. Spectrosc.*, 2016, **94–95**, 11–36.